Transport properties and spin accumulation in semiconductor two-dimensional electron gas/superconductor junctions

Transport properties and spin accumulation in semiconductor two-dimensional electron gas/ superconductor junctions

Guo-Ya Sun

Department of Physics, and Institute of Theoretical Physics and Astrophysics,
Xiamen University, Xiamen 361005, People's Republic of China

Abstract
We extend the Blonder–Tinkham–Klapwijk (BTK) theory to study transport properties of semiconductor two-dimensional electron gas (2DEG)/superconductor junctions, including the Rashbar spin–orbit interaction in a 2DEG of finite width. The effects of Rashba spin–orbit interaction on the conductance are investigated, and a reduction of this conductance is found. A couple of well known results for quantized conductance are verified. Moreover, the averaged spin value and shape of spin fluctuation in the 2DEG are calculated. It is found that the y-component of the spin (S_y) is even, while the x- and z-components are odd, with respect to the propagating mode index. Consequently, S_x and S_z are summed up to vanish, while S_y accumulates to a finite value. S_y is explicitly given and a spin-polarization in the y-direction is found in the 2DEG near the interface.

In recent years there has been a continual increase of interest in spin-dependent electron transport in hybrid structures, aiming at possible applications of electrons' spin (the second degree of freedom apart from the charge) in electronics. This research field is now known as spintronics. Systems comprised of ferromagnets or ferromagnetic semiconductors, in which carriers are spin-polarized, have been studied both extensively and intensively [1–10]. As spin-dependence (spin-polarized) is concerned, however, it does not necessarily always rely on ferromagnetism. More recently, the inverse spin Hall effect, found in semiconductors with a two-dimensional electron gas (2DEG), opened a new area for spin-dependent electron transport [11]. The spin Hall effect, which is actually a kind of dissipationless spin current, was discovered in p-doped zincblende-type semiconductors [12]. Sinova *et al* [13] had also predicted a universal spin Hall conductivity for the 2DEG with Rashba-type spin–orbit interaction (SOI), where spin currents always accompany charge currents. Koga *et al* had reported a spin-filter device using a nonmagnetic resonant tunneling diode, where the Rashba SOI combined with the spin blockade phenomena can enhance the spin-filtering efficiency up to 99.9% [14]. In short, the semiconductor 2DEG, in which spin-polarization may occur both intrinsically and extrinsically,

has received particular attention, and may play an important role in future spintronics.

In general, the Rashba SOI is a result of the up–down asymmetric confining electrostatic potential in the semiconductor heterojunction quantum well, where the 2DEG is located [13, 15]. The Rashba SOI couples the spin degree of freedom to the motion of electrons or holes, and consequently leads to spin splitting of the energy band [16]. Such energy band splitting can be equivalently interpreted as the result of an effective pseudo-magnetic field lying in the plane of the 2DEG. This pseudo-magnetic field is distinguished from a real exchange magnetic field in that it depends on the wavevectors of the electrons or holes, and at the same time does not break the time-inversion symmetry. In narrow-gap InAs semiconductor hybrid structures, for example, the SOI is remarkably strong and leads to a band splitting of about 5 meV between up and down spin directions [17], which is of the same order as the energy gap of conventional superconductors.

It is noted that from the experimental point of view that the 2DEG on a clean InAs surface allows us to create high-quality ohmic contacts with superconductors. Many previous studies on 2DEG/superconductor (SC) hybrid systems concentrated on the effects of the Andreev reflection on electron transport

properties or behaviors of magnetoconductance when an external magnetic field was presented [18–21]. At the same time, the effects of the Rashba SOI on both electron and spin transport were not considered as much. In normal metal/2DEG/normal metal Josephson junctions, as we know, a drastic reduction of the experimentally measured critical current, with respect to the theoretical predictions, is observed [22–24]. Dimitrova *et al* [25] had explored the role of the Rashba SOI in the above case and found that its presence is not sufficient to explain such a reduction. In the present paper, we will theoretically investigate the transport properties of clean semiconductor (2DEG)/SC hybrid junctions, with the focus on effects of the Rashba SOI in the 2DEG and superconductivity of the SC. Differential conductance and average spin value, as well as the shape of the spin fluctuation in the 2DEG are calculated, with proper counting of propagation modes that correspond to a finite width of the 2DEG.

We consider 2DEG/SC junctions as illustrated in the inset of figure 1(b). The 2DEG of width W is located at $x < 0$ and described by the Rashba Hamiltonian, while the superconductor is located at $x > 0$ and described by the conventional Bardeen–Cooper–Schrieffer (BCS) theory, respectively. As is well known, the quasiparticle wavefunction in such systems satisfies the following Bogoliubov–de Gennes (BdG) equation [26, 27]

$$\begin{bmatrix} H_0(\mathbf{r}) & \Delta(\mathbf{r}) \\ \Delta^*(\mathbf{r}) & -H_0(\mathbf{r}) \end{bmatrix} \begin{bmatrix} f_{\mathbf{k}}(\mathbf{r}) \\ g_{\mathbf{k}}(\mathbf{r}) \end{bmatrix} = E \begin{bmatrix} f_{\mathbf{k}}(\mathbf{r}) \\ g_{\mathbf{k}}(\mathbf{r}) \end{bmatrix} \quad (1)$$

where $\Delta(\mathbf{r}) = \Delta_0 \Theta(x)$, with Δ_0 being the superconducting energy gap of the SC at zero temperature. The superconducting energy gap is assumed to be constant in the present paper. E is the quasiparticle energy relative to the Fermi energy level E_F. $f_{\mathbf{k}}(\mathbf{r})$ and $g_{\mathbf{k}}(\mathbf{r})$ are components of the wavefunction. The single particle Hamiltonian $H_0(\mathbf{r})$ is given as

$$H_0(\mathbf{r}) = -\frac{\hbar^2}{2} \nabla \cdot \frac{1}{m(\mathbf{r})} \nabla + U_{SO} + V(x) + V_c(y) - E_F \quad (2)$$

where $m(\mathbf{r}) = m_L^* \Theta(-x) + m_R^* \Theta(x)$, with m_L^* and m_R^* being the effective electron mass in the 2DEG and SC, respectively, and $\Theta(x)$ the unit step function. $U_{SO} = \alpha(\mathbf{r})(\boldsymbol{\sigma} \times \mathbf{p}) \cdot \hat{n}/\hbar$ is the Rashba spin–orbit interaction in the 2DEG, with $\alpha(\mathbf{r}) = \alpha \Theta(-x)$ being the Rashba parameter, $\boldsymbol{\sigma} = (\sigma_x, \sigma_y, \sigma_z)$ are the Pauli matrices, $\mathbf{p}$ is the electron momentum, and $\hat{n}$ is the unit vector normal to the plane of the 2DEG, respectively. $V(x) = V_0 \delta(x)$ is a δ-type potential describing a scattering barrier at the interface ($x = 0$). $V_c(y)$ represents a hard-wall confining potential at the edges of the 2DEG ($y = \pm W/2$) and, consequently, the 2DEG is treated as a quasi-one-dimensional quantum wire with quantized transverse modes. In figure 1, schematic diagrams of (a) propagating waves, where tangential arrows denote spin orientations, and (b) the band structures, are shown. As a general solution of the BdG equation (1), the wavefunction in the whole junction is written as

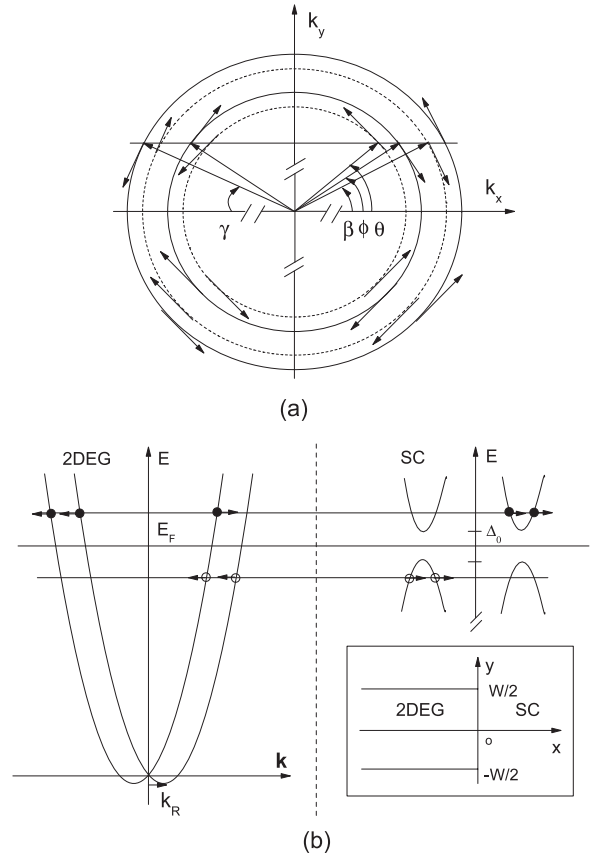$$\Psi_l(\mathbf{r}, s) = \sum_s \psi_l(y) \psi_l^s(x) \quad (3)$$

Figure 1. Schematic diagrams of (a) propagating waves, with tangential arrows denoting spin orientations; and (b) the band structures, with solid (hollow) circles representing electrons (holes) in the 2DEG or ELQ (HLQ) in the SC, respectively. The inset displays the geometry of a 2DEG/superconductor junction system.

where $\psi_l(y) = \sqrt{\frac{2}{W}} \sin[\frac{l\pi}{W}(y + \frac{W}{2})]$, with l being the quantum number which defines the propagating mode, and

$$\psi_l^{s,L}(x) = \begin{pmatrix} 1 \\ 0 \end{pmatrix} e^{ik_l^{s,e}x} \chi_L^{1_s} + b_l^s P \begin{pmatrix} 1 \\ 0 \end{pmatrix} e^{-ik_l^{s,e}x} \chi_L^{b_l^s}$$
$$+ a_l^s \begin{pmatrix} 0 \\ 1 \end{pmatrix} e^{ik_l^{s,h}x} \chi_L^{a_l^s} + b_l^{\bar{s}} \begin{pmatrix} 1 \\ 0 \end{pmatrix} e^{-ik_l^{\bar{s},e}x} \chi_L^{b_l^{\bar{s}}}$$
$$+ a_l^{\bar{s}} \begin{pmatrix} 0 \\ 1 \end{pmatrix} e^{ik_l^{\bar{s},h}x} \chi_L^{a_l^{\bar{s}}} \quad (4)$$

for $x < 0$,

$$\psi_l^{s,R}(x) = c_l^s \begin{pmatrix} u \\ v \end{pmatrix} e^{iq_l^e x} \chi_R^{c_l^s} + d_l^s \begin{pmatrix} v \\ u \end{pmatrix} e^{-iq_l^h x} \chi_R^{d_l^s}$$
$$+ c_l^{\bar{s}} \begin{pmatrix} u \\ v \end{pmatrix} e^{iq_l^e x} \chi_R^{c_l^{\bar{s}}} + d_l^{\bar{s}} \begin{pmatrix} v \\ u \end{pmatrix} e^{-iq_l^h x} \chi_R^{d_l^{\bar{s}}} \quad (5)$$

for $x > 0$. The five terms of $\psi_l^{s,L}$ are waves of incident electrons, normal reflected electrons (b_l^s, $b_l^{\bar{s}}$), and Andreev reflected holes (a_l^s, $a_l^{\bar{s}}$), in the 2DEG, while the four terms of $\psi_l^{s,R}$ are electron-like quasiparticle (ELQ) (c_l^s, $c_l^{\bar{s}}$) and hole-like quasiparticle (HLQ) (d_l^s, $d_l^{\bar{s}}$) waves in the SC, respectively. The superscript $s(= \pm 1)$ is the band index, indicating which band the quasiparticle belongs to, with $\bar{s} = -s$. k_ls and q_ls the x-components of the quasiparticle wavevectors in the

2DEG and SC, respectively. From the dispersion relations $E_s(\mathbf{k}) = \hbar^2[(k + sk_R)^2 - k_R^2]/2m_L^* - (E_F^L + eV)$ in the 2DEG, and $E(\mathbf{q}) = [\Delta^2 + (\hbar^2 q^2/2m_R^* - E_F^R)]^{1/2}$ in the SC, we get the wavevectors explicitly as

$$k^{s,e(h)} = [2m_L^*(E_F^L + eV + \eta_{e(h)}E)/\hbar^2 + k_R^2]^{1/2} - sk_R \quad (6)$$

$$q^{e(h)} = (2m_R^*/\hbar^2)^{1/2}[E_F^R + \eta_{e(h)}(E^2 - \Delta_0^2)^{1/2}]^{1/2} \quad (7)$$

where $k_R = \alpha m_L^*/\hbar^2$, $\eta_{e(h)} = 1(-1)$. The wavevector components parallel to the interface are assumed to remain unchanged during the reflection and transmission processes, i.e. they satisfy the condition,

$$k^{s,e}\sin\phi_l^s = k^{s,h}\sin\theta_l^s = k^{\bar{s},e}\sin\gamma_l^{\bar{s}} = k^{\bar{s},h}\sin\beta_l^{\bar{s}} = k_y \quad (8)$$

χ_Ls are the corresponding spinor functions of the transporting quasiparticles in the 2DEG, which are coupled to the spatial motion via wavevectors and given as

$$\chi_L^{\mathbf{1}_s} = (\mathrm{i}e^{-\mathrm{i}\phi_l^s/2}, e^{\mathrm{i}\phi_l^s/2})^\mathrm{T}/\sqrt{2} \quad (9)$$

$$\chi_L^{b_l^s} = (\mathrm{i}e^{-\mathrm{i}\phi_l'/2}, e^{\mathrm{i}\phi_l'/2})^\mathrm{T}/\sqrt{2} \quad (10)$$

$$\chi_L^{a_l^s} = (-\mathrm{i}e^{-\mathrm{i}\theta_l^s/2}, e^{\mathrm{i}\theta_l^s/2})^\mathrm{T}/\sqrt{2} \quad (11)$$

$$\chi_L^{b_l^{\bar{s}}} = (-\mathrm{i}e^{-\mathrm{i}\gamma_l^{\bar{s}}/2}, e^{\mathrm{i}\gamma_l^{\bar{s}}/2})^\mathrm{T}/\sqrt{2} \quad (12)$$

$$\chi_L^{a_l^{\bar{s}}} = (\mathrm{i}e^{-\mathrm{i}\beta_l^{\bar{s}}/2}, e^{\mathrm{i}\beta_l^{\bar{s}}/2})^\mathrm{T}/\sqrt{2} \quad (13)$$

where $\phi_l^s = \cos^{-1}(k_l^{s,e}/k^{s,e})$, $\phi_l' = \pi - \phi_l^s$, $\theta_l^s = \cos^{-1}(k_l^{s,h}/k^{s,h})$, $\gamma_l^{\bar{s}} = \pi - \cos^{-1}(k_l^{\bar{s},e}/k^{\bar{s},e})$, $\beta_l^{\bar{s}} = \cos^{-1}(k_l^{\bar{s},h}/k^{\bar{s},h})$. All angles are indicated in figure 1(a). The superscript T denotes matrix transposition. χ_Rs are spinor functions in the SC, and, because of the absence of spin–orbit coupling and spin-singlet superconductivity therein, the χ_Rs are assumed to be either spin up or down, as $\chi_R^{c_l^s} = \chi_R^{d_l^{\bar{s}}} = (1 \ 1)^\mathrm{T}/\sqrt{2}$, and $\chi_R^{d_l^s} = \chi_R^{c_l^{\bar{s}}} = (1 \ -1)^\mathrm{T}/\sqrt{2}$. Here, we would like to point out that there must be present diffusive spin scattering at the interface and also in the SC near the interface, to meet the requirements of spin-singlet superconductivity of the SC. Such a diffusive scattering may be interpreted as a kind of proximate effect. Consequently, an accompanying dissipation heating effect may occur and will be investigated elsewhere. The Bogoliubov coherence factors are given as

$$u^2 = 1 - v^2 = \frac{1}{2}\left(1 + \frac{\sqrt{E^2 - \Delta_0^2}}{E}\right). \quad (14)$$

The scattering wavefunction coefficients in equations (3) and (4) can be determined by the boundary condition that ensures the continuity of the electron wavefunction and electronic flux conservation. The boundary conditions in the x-direction are given as

$$\psi_l^{s,L}(0) = \psi_l^{s,R}(0) \quad (15)$$

$$v_x^L\psi_l^{s,L}(0) = v_x^R\psi_l^{s,R}(0) + \frac{2\mathrm{i}V_0}{\hbar}\psi_l^{s,R}(0). \quad (16)$$

Given the above Hamiltonian with SOI interaction (equation (2)), the group velocity of quasiparticles is readily given as

$$\mathbf{v} = \partial H/\partial(\hbar\mathbf{k}) = -\frac{\mathrm{i}\hbar}{m(\mathbf{r})}\nabla - \frac{\alpha(\mathbf{r})}{\hbar}\boldsymbol{\sigma}\times\hat{n}. \quad (17)$$

As a result, their x-components are explicitly given as $v_x^L = -\mathrm{i}(\hbar/m_L^*)\partial/\partial x - \alpha\sigma_y/\hbar$ in the 2DEG, and $v_x^R = -\mathrm{i}(\hbar/m_R^*)\partial/\partial x$ in the SC, respectively. Substituting wavefunction equations (4) and (5) into the boundary condition equations (15) and (16), and after a lengthy algebraic calculation, we have obtained all of the coefficients, which are not explicitly given here because of their lengthy form.

With the definition of the electronic current density

$$\mathcal{J}^e = \mathrm{i}e\hbar/2m_L^*\sum_{s,l}[(\psi_l^{s,L})^\dagger\nabla\psi_l^{s,L} - \psi_l^{s,L}(\nabla\psi_l^{s,L})^\dagger] \quad (18)$$

and following the BTK theory [27], we get differential charge conductance of the 2DEG/SC junctions in the small bias regime as

$$\mathcal{G}_x^e = \frac{2e^2}{h}\sum_{s,l}\left[1 + \frac{v_l^{b_l^s}}{v_l^{\mathbf{1}_s}}|b_l^s|^2 + \frac{v_l^{a_l^s}}{v_l^{\mathbf{1}_s}}|a_l^s|^2 \right.$$
$$\left. + \frac{v_l^{b_l^{\bar{s}}}}{v_l^{\mathbf{1}_s}}|b_l^{\bar{s}}|^2 + \frac{v_l^{a_l^{\bar{s}}}}{v_l^{\mathbf{1}_s}}|a_l^{\bar{s}}|^2\right] \quad (19)$$

where v_ls are x-components of the group velocity of transport quasiparticles in the 2DEG, which are explicitly given as

$$v_l^{\mathbf{1}_s} = \hbar(k_l^{s,e} + k_R\cos\phi_l^s)/m_L^* \quad (20)$$

$$v_l^{b_l^s} = \hbar(-k_l^{s,e} + k_R\cos\phi_l')/m_L^* \quad (21)$$

$$v_l^{a_l^s} = \hbar(k_l^{s,h} - k_R\cos\theta_l^s)/m_L^* \quad (22)$$

$$v_l^{b_l^{\bar{s}}} = \hbar(-k_l^{\bar{s},e} - k_R\cos\gamma_l^{\bar{s}})/m_L^* \quad (23)$$

$$v_l^{a_l^{\bar{s}}} = \hbar(k_l^{\bar{s},h} + k_R\cos\beta_l^{\bar{s}})/m_L^*. \quad (24)$$

It is noted that equation (19) is consistent with the well known results of the BTK theory where the spinor functions were not considered.

In our numerical calculation, we chose parameters analogous to the experimental ones, as $m_L^* = 0.036m_e$, $m_R^* = m_e$, with m_e the mass of an electron, $\Delta_0 = 1.7$ meV, $E_F^L = 37$ meV, $E_F^R = 510$ meV, $\alpha_0 = 10^{-11}$ eV m, and the width $W = 15\pi/k_F^L$ (k_F^L is the Fermi wavevector of the 2DEG for $\alpha = 0$), respectively. It should be noted that the Fermi levels in the 2DEG and SC are aligned for zero bias, while the band bottoms are different, as shown in figures 1. The summation over l in equation (18) is done as follows: for a certain width (W) of the 2DEG, the maximum of l is determined as $l_{\max} = \mathrm{int}(k_f^{s,e}W/\pi)$, for the instance of an electron of band s incidents. All wavevectors and the corresponding incident angles are determined by equation (8), together with the condition that all the k_ys are equal to $l\pi/W$. Then we sum up the contributions of all these modes $[-l_{\max}, l_{\max}]$. In figures 2(a) and (b), the zero-bias differential conductance of the 2DEG/SC junctions is plotted as a function of the incident energy E/Δ_0, with respect to different values
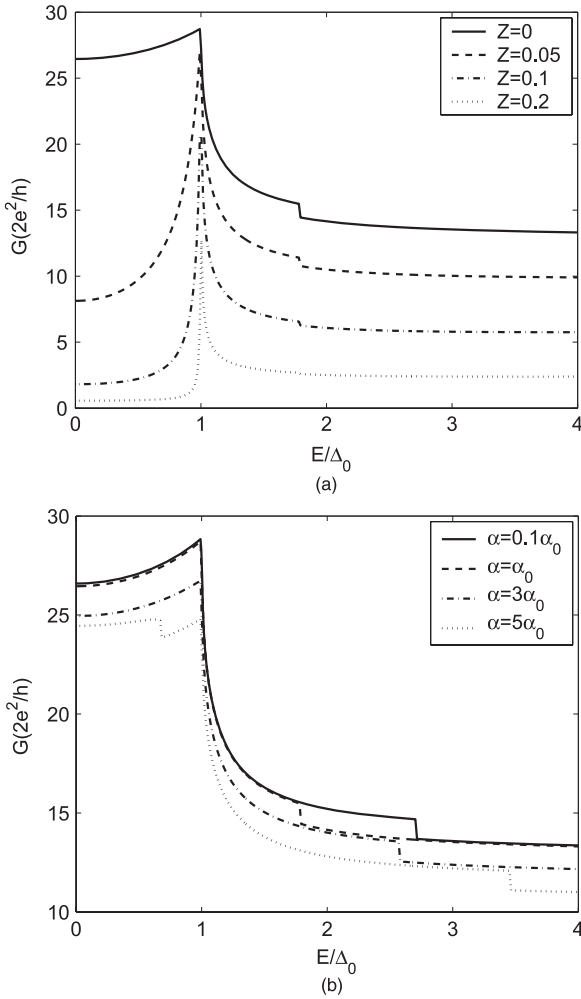
Figure 2. Zero-bias differential conductance of 2DEG/SC junctions, with respect to (a) different interface barrier strength Z and (b) different values of SOI strength α, respectively. With $m_L^* = 0.036 m_e$, $m_R^* = m_e$, $\Delta_0 = 1.7$ meV, $E_F^L = 37$ meV, $E_F^R = 510$ meV, $\alpha_0 = 10^{-11}$ eV m, and $W = 15\pi/k_F^L$.
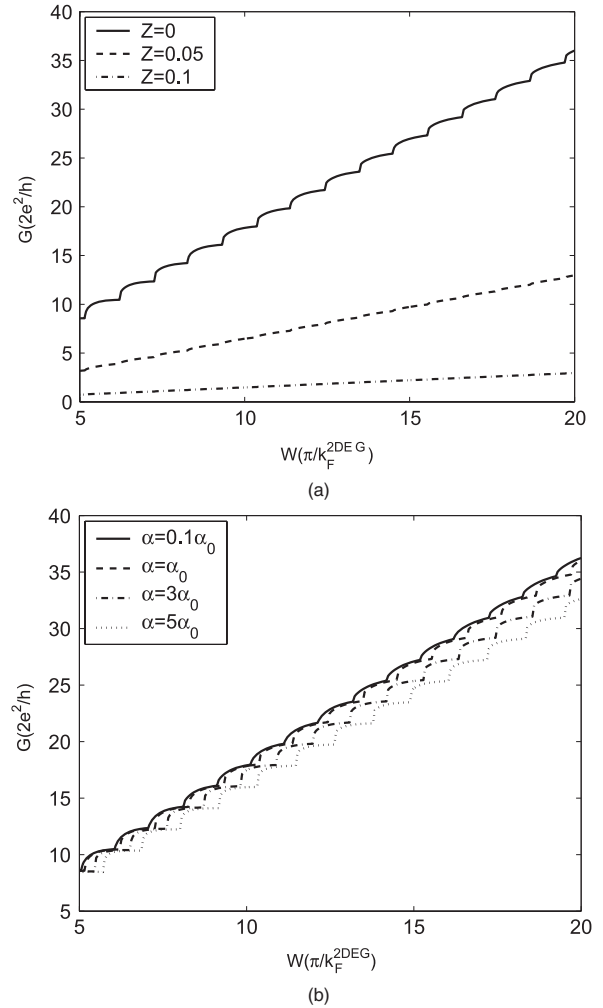
Figure 3. Zero-bias differential conductance as a function of width of the 2DEG for 2DEG/SC junctions, with respect to (a) different interface barrier strength Z and (b) different values of SOI strength α, respectively. With $E = 0.5\Delta_0$ and other parameters the same as in figure 2.

of Z and α, respectively. The superconducting character of the conductance is clearly observed in both the two figures. Figure 2(a) is a result which is similar to several previous works, except for its smaller value of the non-dimensional barrier strength parameter Z ($= 2m_L^* V_0/\hbar^2 q_F$). The smaller Z corresponds to the larger difference between the wavevectors in the 2DEG and SC, for the same interface barrier. Figure 2(b) shows the effect of SOI (denoted by α) in the 2DEG. It is found that the SOI reduces the conductance in general. Such results are consistent with [25]. Moreover, we found that with increasing the quasiparticle energy E and the strength of SOI α, a propagating mode will be blocked, and a sudden reduction (about $2e^2/h$) of G is observed, at some particular points.

In figures 3(a) and (b), we show the zero-bias differential conductance as a function of the width of the 2DEG, where $E = 0.5\Delta_0$ was chosen, and other parameters are the same as in figure 2. Quantized steps of the differential conductance, which correspond to integer numbers of propagating modes with continuous increase of the 2DEG width, are clearly visible. Effects of Z and α are shown in 3(a) and (b), respectively. It is found that the width of a single conductance

step increases with increasing the strength of SOI α, as shown in figure 3(b), which has the same physical meaning as increasing α and may block one or more propagating modes at a certain width of the 2DEG, as shown in figure 2(b).

We now turn our attention to spin transport in the 2DEG. Note that the transport electrons and holes in different bands in the 2DEG generally have non-collinear spin directions, say, depending on the direction of the wavevectors (see figure 1), and the interference between the propagating waves may lead to spin fluctuation and accumulation in the 2DEG. The expectation value of spin in the 2DEG is given as

$$\langle \mathbf{S} \rangle = \sum_{s,l} \int \rho_{s,l}(E) f(E) \langle \Psi_l^L(\mathbf{r}, s) | \boldsymbol{\sigma} | \Psi_l^L(\mathbf{r}, s) \rangle \, \mathrm{d}E \qquad (25)$$

where $\rho_{s,l}(E) = \frac{W}{2\pi\hbar} \sqrt{m_L^*/(E - E_{s,l})}$ is the density of states of electrons in the quasi-one-dimensional 2DEG for each mode, with $E_{s,l} = \hbar^2 k_y^2/2m_L^*$ being the threshold energy of mode l for band s, and $f(E) = [\exp(E/k_B T) + 1]^{-1}$ the Fermi distribution function in the 2DEG. After substituting the wavefunctions, we get
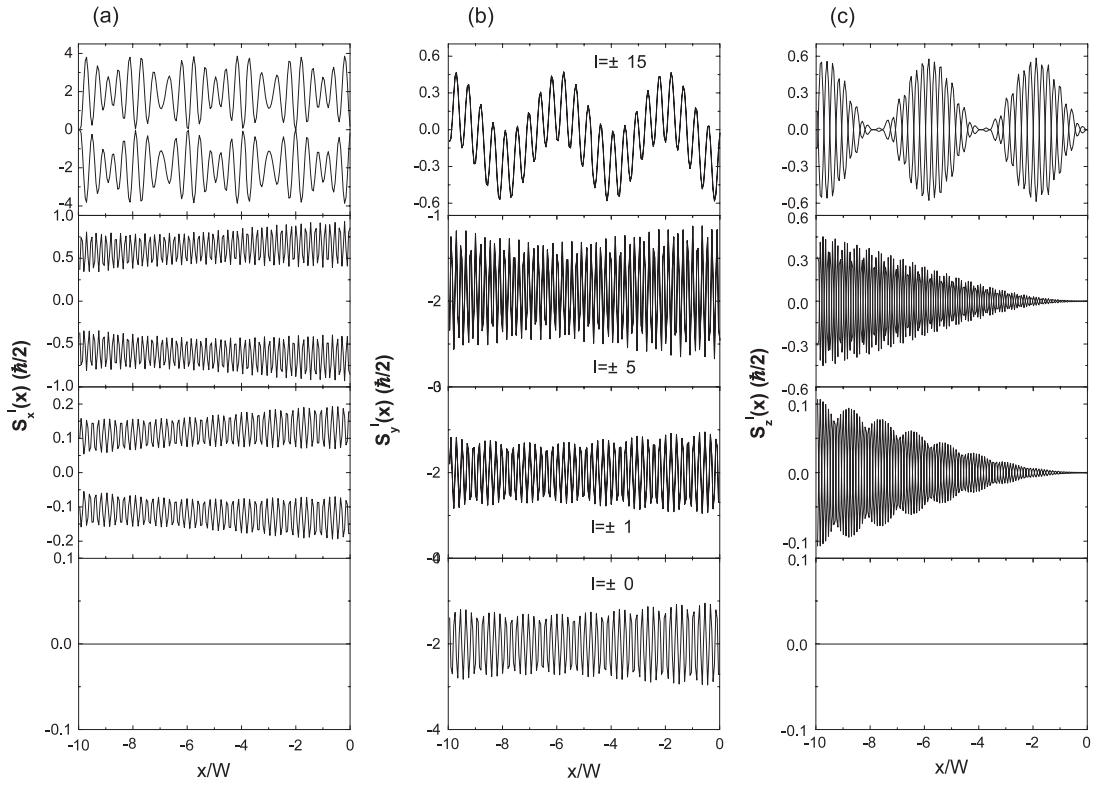
Figure 4. S_i^l ($i = x, y, z$) for several propagating modes as indicated, as a function of longitudinal position in the 2DEG, while columns (a), (b) and (c) correspond to $i = x$, y, and z, respectively. With $eV = 0.5\Delta_0$, $E = 0$, $\alpha = 0.1\alpha_0$, $W = 15\pi/k_F^L$, $Z = 0$, and other parameters the same as in figure 2.
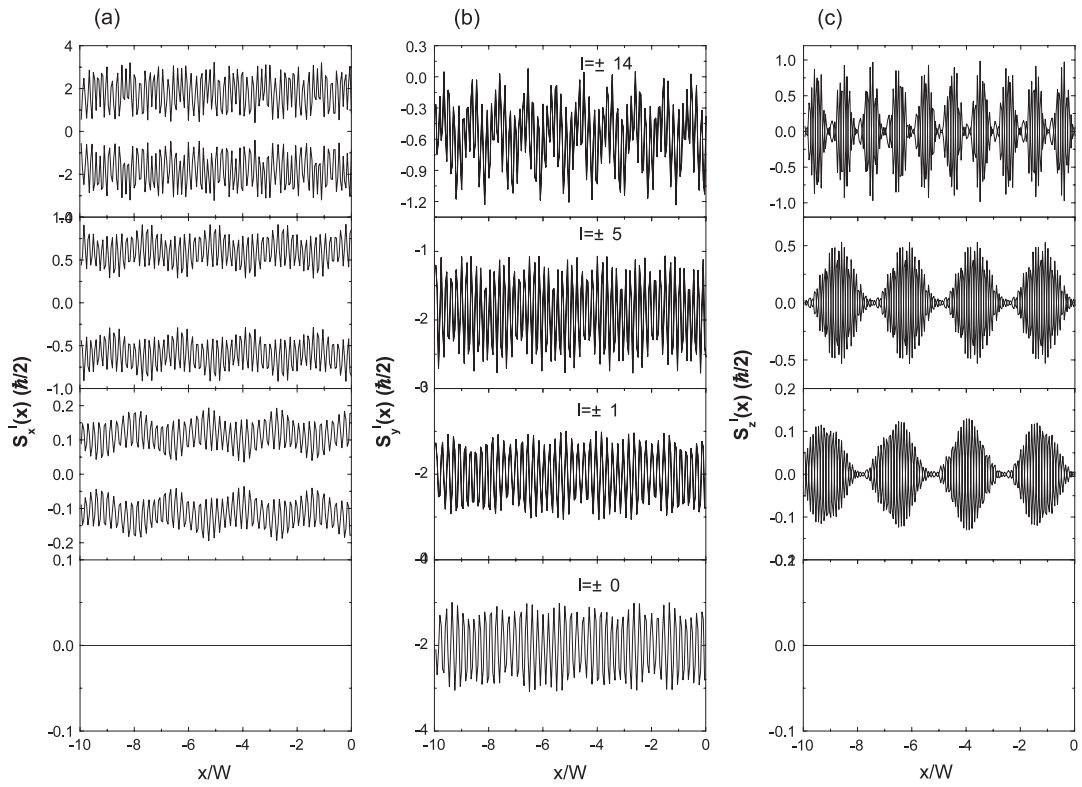

**Figure 5.** The same as in figure 4, except $\alpha = \alpha_0$.

$$\langle S_i(x,y)\rangle = \sum_{s,l} \int \rho_{s,l}(E) f(E) |\psi_l(y)|^2 \langle S_i^{s,l}(x)\rangle \, \mathrm{d}E, \qquad (26)$$

with $i = x, y, z$, and

$$
\begin{aligned}
\langle S_x^{s,l}(x)\rangle = \frac{\hbar}{2}\Bigg\{ & \sin\phi_l^s + |b_l^s|^2 \sin\phi' - |a_l^s|^2 \sin\theta_l^s - |b_l^{\bar{s}}|^2 \\
& \times \sin\gamma_l^{\bar{s}} + |a_l^{\bar{s}}|^2 \sin\beta_l^{\bar{s}} + 2\,\mathrm{Re}\Bigg[b_l^s \mathrm{e}^{-\mathrm{i}2k_l^{s,e}x} + a_l^{\bar{s}} \sin \\
& \times \frac{\beta_l^{\bar{s}}+\phi_l^s}{2}\mathrm{e}^{\mathrm{i}(k_l^{\bar{s},h}-k_l^{s,e})x} + b_l^{s*}a_l^{\bar{s}}\sin\frac{\beta_l^{\bar{s}}+\phi'}{2}\mathrm{e}^{\mathrm{i}(k_l^{s,e}+k_l^{\bar{s},h})x} \\
& - a_l^{s*}b_l^{\bar{s}}\sin\frac{\theta_l^s+\gamma_l^{\bar{s}}}{2}\mathrm{e}^{-\mathrm{i}(k_l^{s,e}+k_l^{\bar{s},e})x}\Bigg] + 2\,\mathrm{Im}\Bigg[a_l^s\cos\frac{\phi_l^s+\theta_l^s}{2} \\
& \times \mathrm{e}^{\mathrm{i}(k_l^{s,h}-k_l^{s,e})x} + b_l^{\bar{s}}\cos\frac{\phi_l^s+\gamma_l^{\bar{s}}}{2}\mathrm{e}^{-\mathrm{i}(k_l^{s,e}+k_l^{\bar{s},e})x} \\
& + b_l^{s*}a_l^s\cos\frac{\theta_l^s+\phi'}{2}\mathrm{e}^{\mathrm{i}(k_l^{s,e}+k_l^{s,h})x} \\
& + b_l^{s*}b_l^{\bar{s}}\cos\frac{\phi'+\gamma_l^{\bar{s}}}{2}\mathrm{e}^{\mathrm{i}(k_l^{s,e}-k_l^{\bar{s},e})x} + a_l^{\bar{s}*}a_l^s\cos\frac{\theta_l^s+\beta_l^{\bar{s}}}{2} \\
& \times \mathrm{e}^{\mathrm{i}(k_l^{s,h}-k_l^{\bar{s},h})x} + a_l^{\bar{s}*}b_l^{\bar{s}}\cos\frac{\beta_l^{\bar{s}}+\gamma_l^{\bar{s}}}{2}\times\mathrm{e}^{-\mathrm{i}(k_l^{\bar{s},e}+k_l^{\bar{s},h})x}\Bigg]\Bigg\} \quad (27)
\end{aligned}
$$

$$
\begin{aligned}
\langle S_y^{s,l}(x)\rangle = \frac{\hbar}{2}\Bigg\{ & -\cos\phi_l^s - |b_l^s|^2\cos\phi' + |a_l^s|^2\cos\theta_l^s \\
& + |b_l^{\bar{s}}|^2\cos\gamma_l^{\bar{s}} - |a_l^{\bar{s}}|^2\cos\beta_l^{\bar{s}} + 2\,\mathrm{Re}\Bigg[-a_l^s\cos\frac{\beta_l^{\bar{s}}+\phi_l^s}{2} \\
& \times \mathrm{e}^{\mathrm{i}(k_l^{\bar{s},h}-k_l^{s,e})x} - b_l^{s*}a_l^{\bar{s}}\cos\frac{\beta_l^{\bar{s}}+\phi'}{2}\mathrm{e}^{\mathrm{i}(k_l^{s,e}+k_l^{\bar{s},h})x} \\
& + a_l^{s*}b_l^{\bar{s}}\cos\frac{\theta_l^s+\gamma_l^{\bar{s}}}{2}\mathrm{e}^{-\mathrm{i}(k_l^{\bar{s},e}+k_l^{s,h})x}\Bigg] + 2\,\mathrm{Im}\Bigg[a_l^s\sin\frac{\phi_l^s+\theta_l^s}{2} \\
& \times \mathrm{e}^{\mathrm{i}(k_l^{s,h}-k_l^{s,e})x} + b_l^{\bar{s}}\sin\frac{\phi_l^s+\gamma_l^{\bar{s}}}{2}\mathrm{e}^{-\mathrm{i}(k_l^{s,e}+k_l^{\bar{s},e})x} \\
& + b_l^{s*}a_l^s\sin\frac{\theta_l^s+\phi'}{2}\mathrm{e}^{\mathrm{i}(k_l^{s,e}+k_l^{s,h})x} + b_l^{s*}b_l^{\bar{s}}\sin\frac{\phi'+\gamma_l^{\bar{s}}}{2} \\
& \times \mathrm{e}^{\mathrm{i}(k_l^{s,e}-k_l^{\bar{s},e})x} + a_l^{\bar{s}*}a_l^s\sin\frac{\theta_l^s+\beta_l^{\bar{s}}}{2}\mathrm{e}^{\mathrm{i}(k_l^{s,h}-k_l^{\bar{s},h})x} \\
& + a_l^{\bar{s}*}b_l^{\bar{s}}\sin\frac{\beta_l^{\bar{s}}+\gamma_l^{\bar{s}}}{2}\mathrm{e}^{-\mathrm{i}(k_l^{\bar{s},e}+k_l^{\bar{s},h})x}\Bigg]\Bigg\} \quad (28)
\end{aligned}
$$

$$
\begin{aligned}
\langle S_z^{s,l}(x)\rangle = -\frac{\hbar}{2}\Bigg\{ & 2\,\mathrm{Re}\Bigg[a_l^s\cos\frac{\phi_l^s-\theta_l^s}{2}\mathrm{e}^{\mathrm{i}(k_l^{s,h}-k_l^{s,e})x} \\
& + b_l^{\bar{s}}\cos\frac{\phi_l^s-\gamma_l^{\bar{s}}}{2}\mathrm{e}^{-\mathrm{i}(k_l^{s,e}+k_l^{\bar{s},e})x} + b_l^{s*}a_l^s\cos\frac{\phi'-\theta_l^s}{2} \\
& \times \mathrm{e}^{\mathrm{i}(k_l^{s,e}+k_l^{s,h})x} + b_l^{s*}b_l^{\bar{s}}\cos\frac{\phi'-\gamma_l^{\bar{s}}}{2}\mathrm{e}^{\mathrm{i}(k_l^{s,e}-k_l^{\bar{s},e})x} \\
& + a_l^{s*}a_l^{\bar{s}}\cos\frac{\theta_l^s-\beta_l^{\bar{s}}}{2}\mathrm{e}^{\mathrm{i}(k_l^{\bar{s},h}-k_l^{s,h})x} + b_l^{\bar{s}*}a_l^{\bar{s}}\cos\frac{\gamma_l^{\bar{s}}-\beta_l^{\bar{s}}}{2} \\
& \times \mathrm{e}^{\mathrm{i}(k_l^{\bar{s},e}+k_l^{\bar{s},h})x}\Bigg] + 2\,\mathrm{Im}\Bigg[b_l^s\sin\frac{\phi_l^s-\phi'}{2}\mathrm{e}^{-\mathrm{i}2k_l^{s,e}x} \\
& + a_l^{\bar{s}}\sin\frac{\phi_l^s-\beta_l^{\bar{s}}}{2}\mathrm{e}^{\mathrm{i}(k_l^{\bar{s},h}-k_l^{s,e})x} + b_l^{s*}a_l^{\bar{s}}\sin\frac{\phi'-\beta_l^{\bar{s}}}{2} \\
& \times \mathrm{e}^{\mathrm{i}(k_l^{s,e}+k_l^{\bar{s},h})x} + a_l^{s*}b_l^{\bar{s}}\sin\frac{\theta_l^s-\gamma_l^{\bar{s}}}{2}\mathrm{e}^{-\mathrm{i}(k_l^{s,h}+k_l^{\bar{s},e})x}\Bigg]\Bigg\}.
\end{aligned}
$$
$$(29)$$
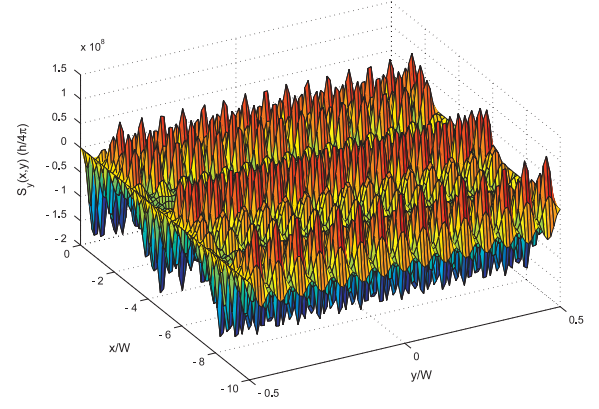
(a)
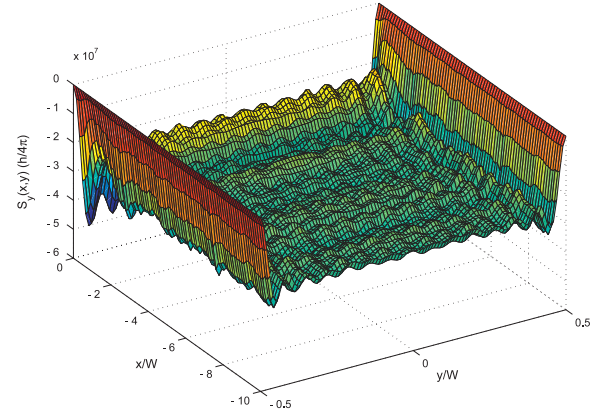
(b)

Figure 6. Spin value S_y, after summing up all propagating modes and integrating over E, for each position in the 2DEG, with $kT = 0.5\Delta_0$, while (a) and (b) correspond to $\alpha = 0.1\alpha_0$ and α_0, respectively. The other parameters are identical to those in figure 4.

(This figure is in colour only in the electronic version)

It is clearly visible that there exist contributions to the expectation value of spin accumulation from both the individual wave components and the interference between them.

We first study the behavior of each propagating mode. In figure 4, $S_i^l(x) = \sum_s S_i^{s,l}(x)$ $(i = x, y, z)$ are given for each mode as a function of longitudinal position in the 2DEG, with $eV = 0.5\Delta_0$, $E = 0$, and $\alpha = 0.1\alpha_0$, while columns (a), (b) and (c) correspond to $i = x, y$, and z, respectively. For the sake of clarity, we just show a couple of selected propagating modes as indicated. The rapid oscillation and long range fluctuation result from the interference terms such as $\exp[\mathrm{i}(k_l^{s,e} + k_l^{\bar{s},h})x]$ and $\exp[\mathrm{i}(k_l^{s,e} - k_l^{\bar{s},e})x]$, respectively, as they appear in equations (27)–(29). It is clearly shown that S_y^l is even, while S_x^l and S_z^l are odd, with respect to the mode index from $-l_{\max}$ to $l_{\max}$. Figure 5 shows the same results as in figure 4, but now $\alpha = \alpha_0$. The effects of different strengths of SOI are found in α-dependent wavevectors, as contained in equation (6). It is found that $l_{\max}$ equals 15 for $\alpha = 0.1\alpha_0$, and 14 for $\alpha = \alpha_0$, respectively, for identical width of the 2DEG, $W = 15\pi/k_F^L$.

Therefore, after summing up contributions of all modes and integrating over incident energy E of the quasiparticles, S_y reaches a finite and observable value, while at the same time, S_x and S_z vanish. That is, the expectation value of spin accumulation has only the y-component, and the quasiparticles in the 2DEG are spin-polarized in the y-direction. Such a spin-polarization may be attributed to an electronic current along the x-direction in the 2DEG (having the same effect as an electronic field along the x-direction), while the detailed shape of spin accumulation is determined by factors such as geometrical dimensions of the sample, the strength of the electronic field, as well as detailed properties of the SOI in the 2DEG. In figure 6, S_y is plotted in the 2DEG near the interface, from $x = 0$ to $-10W$. The spin amplitude for each site is shown. For weaker SOI of (a) $\alpha = 0.1\alpha_0$, it is obvious that S_y has both values of $\pm\hbar/2$, while components of $-\hbar/2$ have a small priority over the $\hbar/2$ ones. For (b) $\alpha = \alpha_0$, however, S_y has only the $-\hbar/2$ component, which means that a complete spin-polarization along the y-direction occurs. We would like to point out that zero spin accumulation exactly at the edges ($y = \pm W/2$) is a result of vanishing wavefunctions there, in the hard-wall model.

In summary, we have studied quasiparticle transport properties in 2DEG/SC junctions, where the 2DEG is of finite width and with Rashba spin–orbit interaction taken into account. The behavior of transporting quasiparticles in such a system is described by the BdG equation. Spinor functions of quasiparticles in the 2DEG which depend on the wavevectors, and those in the SC which are assumed to be either up or down, are all explicitly given. Effects of the Rashba SOI on the conductance are investigated in detail and a couple of well known results of quantized conductance are verified. Moreover, the spin accumulation in the 2DEG is calculated. It is found that S_y is even, while S_x and S_z are odd, with respect to the propagating mode index. Consequently, S_x and S_z are summed up to be vanishing, while a non-zero S_y remains in the 2DEG near the interface.

Acknowledgments

References

[1] Baibich M N, Broto J M, Fert A, Nguyen Van Dau F, Petroff F, Etienne P, Creuzet G, Friederich A and Chazelas J 1988 *Phys. Rev. Lett.* **61** 2472

[2] Binasch G, Grunberg P, Saurenbach F and Zinn W 1989 *Phys. Rev. B* **39** 4828

[3] Moodera J S, Kinder L R, Wong T M and Meservey R 1995 *Phys. Rev. Lett.* **74** 3273

[4] Gallagher W J, Parkin S S P, Lu Y, Bian X P, Marley A, Poche K P, Altman R A, Rishton S A, Jahnes C, Shaw T M and Xiao G 1997 *J. Appl. Phys.* **81** 3741

[5] Fiederling R, Keim M, Reuscher G, Ossau W, Schmidt G, Waag A and Molenkamp L W 1999 *Nature* **402** 787

[6] Zhu J-X, Friedman B and Ting C S 1999 *Phys. Rev. B* **59** 9558–63

[7] Ohno Y, Young D K, Beschoten B, Matsukura F, Ohno H and Awschalom D D 1999 *Nature* **402** 790

[8] Zhu H J, Ramsteiner M, Kostial H, Wassermeier M, Schonherr H-P and Ploog K H 2001 *Phys. Rev. Lett.* **87** 016601

[9] Maekawa S and Shinjo T (ed) 2002 *Spin Dependent Transport in Magnetic Nanostructures* (London: Taylor and Francis)

[10] Zutic I, Fabian J and Das Sarma S 2004 *Rev. Mod. Phys.* **76** 323–410

[11] Engel H, Rashba E I and Halperin B I 2006 *Preprint* cond-mat/0603306
Scheliman J 2006 *Int. J. Mod. Phys.* B **20** 1015

[12] Murakami S, Nagaosa N and Zhang S C 2003 *Science* **301** 1348

[13] Sinova J, Culcer D, Niu Q, Sinitsyn N A, Jungwirth T and MacDonald A H 2004 *Phys. Rev. Lett.* **92** 126603

[14] Koga T, Nitta J, Akazaki T and Takayanagi H 2002 *Phys. Rev. Lett.* **89** 046801
Koga T, Nitta J, Takayanagi H and Datta S 2002 *Phys. Rev. Lett.* **88** 126601

[15] Rashba E I 1960 *Fiz. Tverd. Tela* **2** 1224
Rashba E I 1960 *Sov. Phys.—Solid State* **2** 1109

[16] Molenkamp L W, Schmidt G and Bauer G E W 2001 *Phys. Rev. B* **64** 121202(R)

[17] Nitta J, Akazaki T, Takayanagi H and Enoki T 1997 *Phys. Rev. Lett.* **78** 1335

[18] Asano Y and Yuito T 2000 *Phys. Rev. B* **62** 7477

[19] Takagaki Y 1998 *Phys. Rev. B* **57** 4009

[20] Castellana C, Giazotto F, Governale M, Taddei F and Beltram F 2006 *Appl. Phys. Lett.* **88** 052502

[21] de Jong M J M and Beenakker C W J 1995 *Phys. Rev. Lett.* **74** 1657

[22] Chrestin A, Matsuyama T and Merkt U 1997 *Phys. Rev. B* **55** 8457

[23] Schapers Th, Guzenko V A, Muller R P, Golubov A A, Brinkman A, Crecilius G, Kaluza A and Luth H 2003 *Phys. Rev. B* **67** 014522

[24] Ebel M, Busch C, Merkt U, Grajcar M, Plecenik T and Ilichev E 2005 *Phys. Rev. B* **71** 052506

[25] Dimitrova O and Feigel'man M V 2005 *Preprint* cond-mat/0510182

[26] de Gennes P G 1966 *Superconductivity of Metals and Alloys* (New York: Benjamin)

[27] Blonder G E, Tinkham M and Klapwijk T M 1982 *Phys. Rev. B* **25** 4515